Military Technical College
Kobry El-Kobbah,
Cairo, Egypt.

15th International Conference on Applied Mechanics and Mechanical Engineering.

COMPUTATIONAL ANALYSIS OF A TRUSS TYPE FUSELAGE

I. A. Yousif*, M. A. M. Zein** and M. E. Elsayed***

ABSTRACT

The strength of a welded truss type fuselage of a light aircraft is considered in this paper. The fuselage geometry has been extracted experimentally from a built one and modeled using a CAD package. Aerodynamic loads have been determined using standard loading calculations accepted in the industry.

Static structural analysis has been conducted using finite element method FEM for the rear section of fuselage with great consideration to welding complexity. The result has been found acceptable but further experimental validation is needed. Presently experimental and dynamic analysis is being conducted and the results will be published later.

KEY WORDS

Structural analysis, static analysis, truss, rear fuselage.

* M. Sc. Student, Karary University. Email address: smileyousif@gmail.com.
** B. Sc. Khartoum univ., Mechanical Eng. Dept. Email address: mageedoo@windowslive.com.
*** Assist. Prof., Karary Univ., Aeronautical Dept. Email address: mohadi20@hotmail.com.

NOMENCLATURE

JAR-VLA	Joint aviation regulation – Very light aircraft
W	The Weight of aircraft
S	The wing area
n	The load factor
$\overline{w}$	Load distribution
$H_y^p(y)$	Lift distribution
a	Lift distribution in (y) section
b	Span length
C	Chord length
Sub H	Horizontal
Sub V	Vertical

INTRODUCTION

The aircraft is a light monoplane with high strut-braced wings equipped with flaps. The fuselage is of welded tubular steel fabric-covered construction. The pilots' compartment enclosure is covered with transparent plastic sheets on the top and sides. The fixed split-v type landing gear incorporates individually sprung, hydraulic brake equipped wheels. The wheels are mounted by low-pressure 8.00× 4-inch tires. The steerable 8 × 3.00 tail wheel is mounted on steel spring leaves. Tail surfaces are conventional, with a manually controlled adjustment provided for the stabilizer as shown in Fig. 1, Fig. 2 and Fig. 3.

According to its production contract, SAFAT01 is fully produced and assembled in Sudan whereas the documentation was limited to technical side only with no information available concerning design procedures and calculations as in Fig. 4. This makes it impossible to further modify or upgrade the aircraft. Therefore some kind of reverse engineering has to be adopted; this includes modeling of the aircraft. Then analyzing it computationally and experimentally. In this paper the rear fuselage truss which is loaded by tail air loads has been considered. The fuselage bulkhead at the attach-points station is heavy enough so that it may be assumed to be rigid in its own plane. Hence, the truss may be analyzed as cantilevered as shown in Fig. 5.

3-D MODELING

The 3-D modeling of the fuselage has been obtained from the maintenance manual 3- view as illustrated in Fig. 2. Also actual fuselage truss has been considered in modeling process as in Fig. 3.

2-D drawings were the provider for basic dimensions data as illustrated in Fig. 4. The fuselage skeleton has been drawn as lines first, to ensure the centers of bars are in the accurate position. Second step was configuring the rods as surfaces; the benefit of these surfaces is to simplify the difficulty of joining two cylinders together.

Finally the intended shape has been completed as a solid assembly by drawing every rod as a separate part; the separation has been done to facilitate the manufacturing processes by drafting each part and supplying it to manufacturer or directly feeding the drawing to CNC machine. Fig.6. unveils the complete drawing of SAFAT 01 truss.

AERODYNAMIC LOADING

Aerial structures should possess two features, high strength and low weight. That means, an accurate loading is required, i.e. wind tunnel test data. But in this case the standard loads have been applied namely JAR-VLA as wind tunnel data was not available. For purposes of simplifying the problem, only the rear of fuselage has been considered in the analysis, the applied load is from pressure distribution around fuselage and aerodynamic loads from horizontal and vertical tail stabilizers and also tail landing gear.

The JAR-VLA appendix (A) described the method which can be used to calculate the loads on fuselage. In this method, using parameter ($n\frac{W}{S}$), the load distribution along the chord of each section of vertical or horizontal tails can be drawn. The area under the curve of each section was equal to the amount of distributed load in that section, so the amount of distributed load on the root of each horizontal or vertical tails could be obtained.

Load distribution along the chord in the section of horizontal and vertical tail's root was drawn based on the abovementioned method.

$n = 3.8 \quad W = 700\ (kg) \quad S = 15.87\ (m^2) \quad n\frac{W}{S} = 167.6\ (\frac{kg}{m^2})$

$$\bar{w} = 4.8 + .109(n\frac{W}{S}) \tag{1}$$

Figure 8 shows the distributed load for horizontal tail

$\bar{w} = 23.07\ (\frac{kg}{m^2}), \quad H_y^p(y) = 26.92\ (kg/m)$

Also for vertical tail, Fig.9 shows the distributed load

$\bar{w} = 31.46\ (\frac{kg}{m^2}) \quad H_y^p(y) = 31.46\ (kg/m)$

Load distribution along tails span-wise is elliptical shape. The amount of distributed load on any section of horizontal and vertical tails can be calculated by elliptical equation.

$$\frac{y^2}{b^2} + \frac{H_y^p(y)^2}{a^2} = 1 \tag{2}$$

$b_H = 2.884\ (m)$

$$\frac{y^2}{1.442^2} + \frac{H_{z\,hor}^p(y)^2}{26.922^2} = 1 \tag{3}$$

$b_V = 1.134\ (m)$

$$\frac{y^2}{1.134^2} + \frac{H_y^p(y)^2}{31.46^2} = 1 \tag{4}$$

Tails Force Calculations

After determining aerodynamic load distribution, shearing force of each section of tails can be obtained from equation (5):

$$Q_z^p(y) = \int_{0.5b_H}^{z} H_z^p(y)dy\ (kg) \tag{5}$$

Bending and twist distribution moment can also be determined by following relationships (6) and (7):

$$m_b^p(y) = -H_Z^p(y) * \left(X_{o,j}(y) - X_{c.p}(y)\right) * \sin\emptyset\ \ (kg) \tag{6}$$

$$m_t^p(y) = H_Z^p(y) * \left(X_{o,j}(y) - X_{c.p}(y)\right) * \cos\emptyset\ \ (kg) \tag{7}$$

The configurations of horizontal and vertical stabilizers have elliptical shape and it was difficult to calculate the forces and moments. To solve this problem an alternative and analog shape with equal area and symmetrical main axis has been used as illustrated in Fig. 10 and Fig. 11.

The stiffness center in every section can be expressed in (8):

$$X_{o,j}(y) = 0.33C(y) \quad (m) \tag{8}$$

Also the aerodynamic center as in (9):

$$X_{c.p}(y) = 0.25C(y) \quad (m) \tag{9}$$

The sweep angle of horizontal tail at quarter chord $\emptyset = 7^\circ$
The sweep angle of vertical tail at quarter chord $\emptyset = 21^\circ$

At the last, bending and twist moments in each section of horizontal and vertical tails can be determined by integrating the distributed moments for horizontal and vertical tails:

$$M_b^p(y) = \int_{0.5b}^{y} [\frac{Q_z^p(y)}{\cos\emptyset} + m_b^p(y)\,]\,dy\ (kg.m) \quad (10)$$

$$M_t^p(y) = \int_{0.5b}^{y} [m_t^p(y)]dy\ \ (kg.m) \quad (11)$$

Finally the fuselage will support the tail surfaces at the attachments which coincide approximately at root chord of these surfaces. Thus shear force, bending moment and twisting moment will be taken from root at (y) =0 as detailed in Fig. 12 through Fig. 19. Tail landing gear weight was considered as concentrated load as described in Table1.

The aerodynamic loads, namely pressure distribution, can be neglected in comparison to tail forces and moments in the rear section.

STRUCTURAL ANALYSIS

The first of the analysis of multi-parts model may be the definition of the connections between the parts of the assembly, in this case fastened connection was chosen. *Octree tetrahedron* mesh – parabolic type- was selected for this solid model, the size of the element was 2mm and the absolute sag was 1mm as described in Fig. 20, Table 2, Table 3 and Table 4.

Section A as shown in Fig. 5 was assumed to be rigid so the faces of the tubes at this section were clamped.

The maximum values of shear, bending and torsion loads, resulted from the tails forces and moments calculation, have been applied on the attachment area with fuselage as detailed in Table 5.

RESULTS

Contour plots allow to clearly discussing the various output solutions. The maximum displacement was found 3.17 mm at the tip of the vertical tube where vertical stabilizer is attached to the fuselage. This value is however aerodynamically and structurally acceptable as detailed in Fig. 21.

Principal stresses of range between 4.48*108 to -5.7*108 have been measured as in Fig. 22. The magnitude of the Von Mises stress as illustrated in Fig. 22 indicates that the value of stress varies from $2.93*10^3$ to $4.74*10^7$ N/m^2 for the whole rear section of fuselage truss. But stress concentration of large value namely $4.74*10^8$ N/m^2 has been found at the joint between the vertical support tube and horizontal support tube which exceeds the yield limit of steel which was $2.5*10^8$ N/m^2 as in Fig.23.

CONCLUSION AND RECOMMENDATION

Modeling of truss fuselage as 3-D has been done accurately and loads have been extracted from horizontal and vertical stabilizers which were supported by the section of fuselage truss. The type and size of the mesh elements were chosen in preprocessing phase to be *Octree tetrahedron* mesh (parabolic type), 2mm respectively.

The maximum displacement was found 3.17 mm at the tip of the vertical tube where vertical stabilizer is attached to the fuselage. This value is however aerodynamically and structurally namely for welding joint is acceptable, The range of Von Mises stress value is between $2.93*10^3$ to $4.74*10^7$ N/m^2 which yields quite enough safety margin for welded joints when compared with yield stress of $2.5*10^8$ N/m^2

Analysis results were satisfactory and reasonable for static analysis case; although some spots of high stress concentration have been detected as illustrated in Fig. 23 which could be managed by strengthening the corner edge using filleting techniques to reduce the stress concentration. However, this requires more verification which will be fulfilled by experimental tests.

REFERENCES

[1] JAR-VLA. Joint Aviation Regulation,-Very Light Aircraft, European standard, April 2009.

[2] Bruhn, E. F, "Analysis and design of flight vehicle structures ", Jacobs Publishers, 10585 N. Meridian St., Suite 220, Indianapolis, IN 46290, 1975.

[3] Design and Fabrication of Ultra-light Aircraft Using in Country Resources College of aeronautical engineering PAF academy, RISALPUR 03 September 2010. http://www.scribd.com/doc/37134859/40/Figure-23-Fuselage-Truss-dimensions.

TABLES AND FIGURES

Table1. Loads applied on rear truss.

Item	Shear Force (N)	Bending Moment (N.m)	Twist Moment (N.m)
Horizontal Tail	294.98	56.056	3.528
Vertical Tail	271.46	31.36	3.822
Tail landing Gear	78.4	-	-

Table 2. Mesh.

Entity	Size
Nodes	5134226
Elements	2593345

Table 3. Element Type.

Connectivity	Statistics
Te10	2581491 (99.54%)
Spider	11854 (0.46%)

Table 4. Element Quality.

Criterion	Good	Poor	Bad	Worst	Average
Stretch	2581441 (100.00%)	50 (0.00%)	0 (0.00%)	0.189	0.598
Aspect Ratio	2386699 (92.45%)	194676 (7.54%)	116 (0.00%)	5.916	2.038

Table 5. Materials properties**.**

Material	Steel
Young's modulus	2e+011 N/m^2
Poisson's ratio	0.266
Density	7860 kg/m^3
Coefficient of thermal expansion	1.17e-005 1/Kdeg
Yield strength	2.5e+008 N/m^2

Fig.1. Actual airplane.

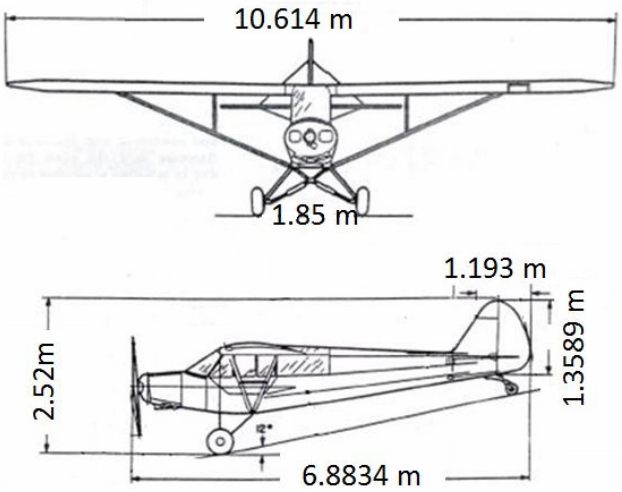

Fig.2. Three view of the aircraft.

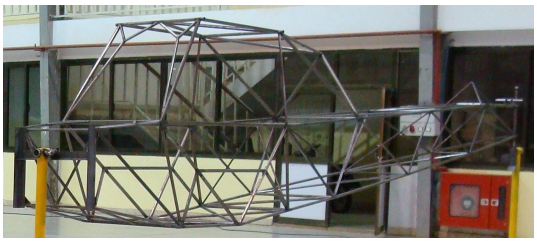

Fig.3. Actual truss.

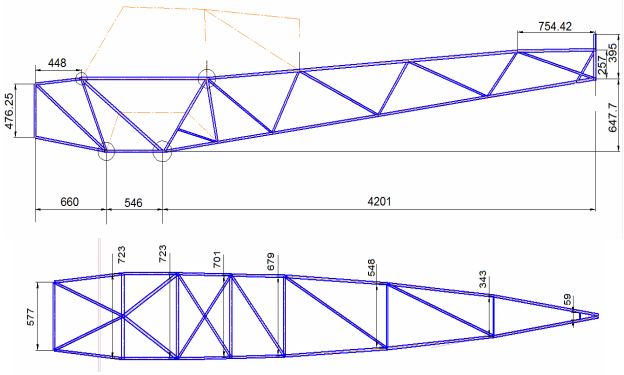

Fig.4. Fuselage 2D drawing.

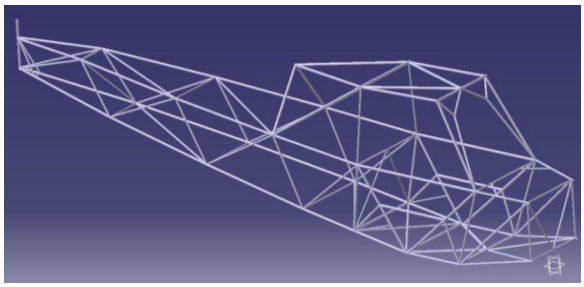

Fig.5. Truss 3D drawing.

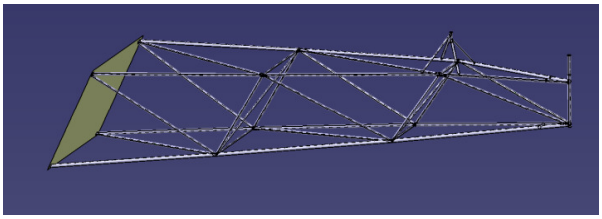

Fig.6. Rear section of the fuselage.

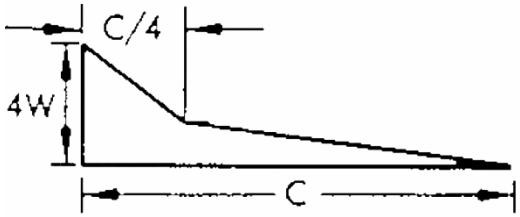

Fig.7. Chord-wise distribution of tail surfaces.

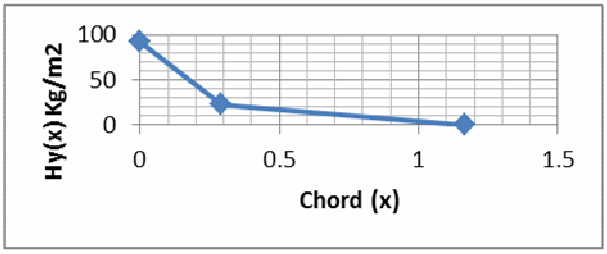

Fig.8. Chord-wise Load distribution along the horizontal tails root section.

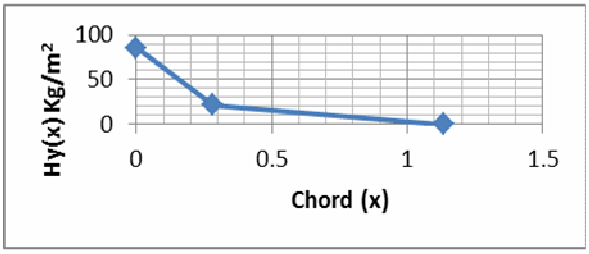

Fig.9. Chord-wise Load distribution along the vertical tails root section.

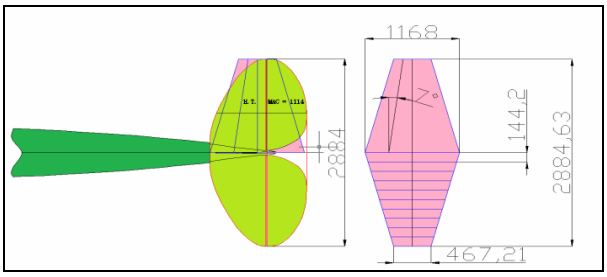

Fig.10. Geometric scheme of horizontal tails.

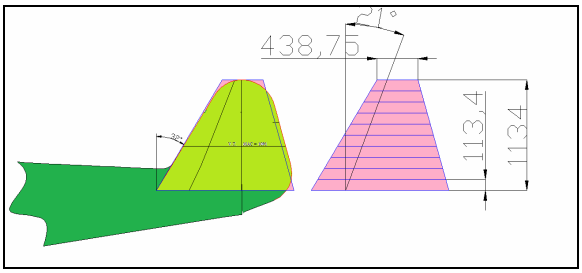

Fig.11. Geometric scheme of vertical tails.

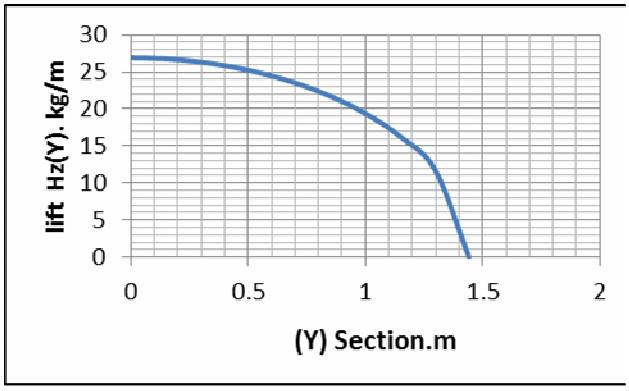

Fig.12. Span-wise lift distribution on horizontal tails.

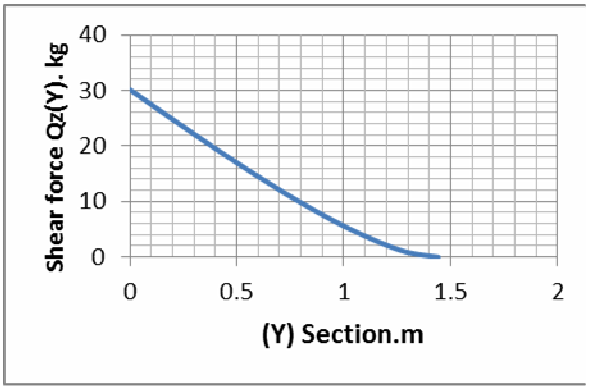

Fig.13. Span-wise shear force distribution on horizontal tails.

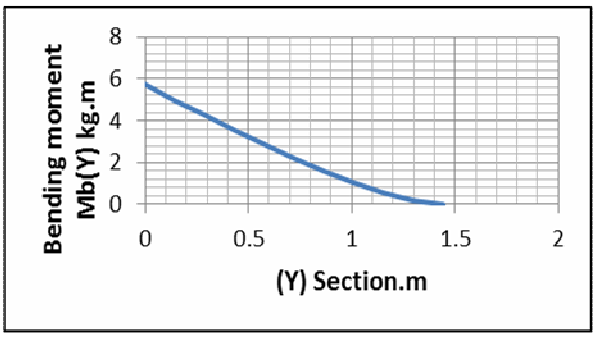

Fig.14. Span-wise Bending moment distribution on horizontal tails.

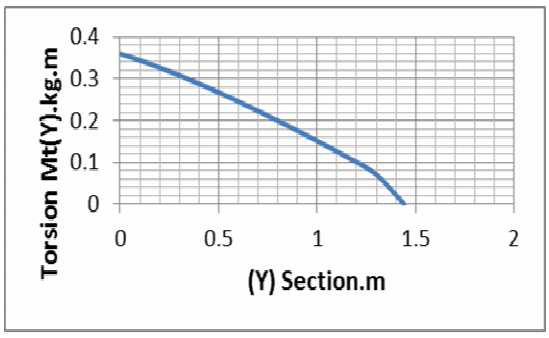

Fig.15. Span-wise torsion moment distribution on horizontal tails.

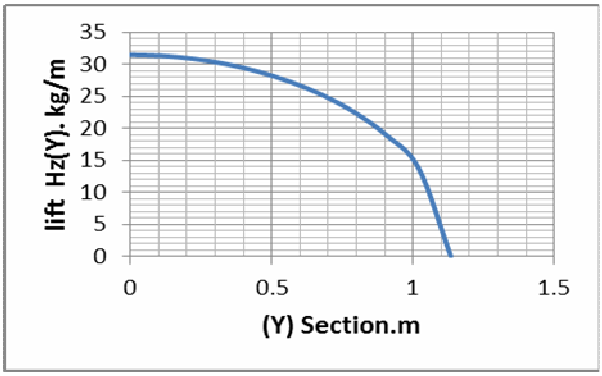

Fig.16. Span-wise lift distribution vertical tails.

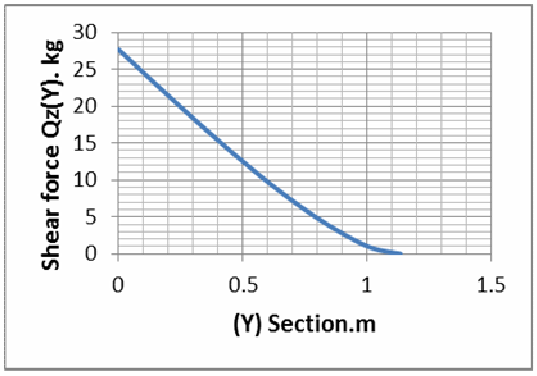

Fig.17. Shear force distributed on span on wise vertical tails.

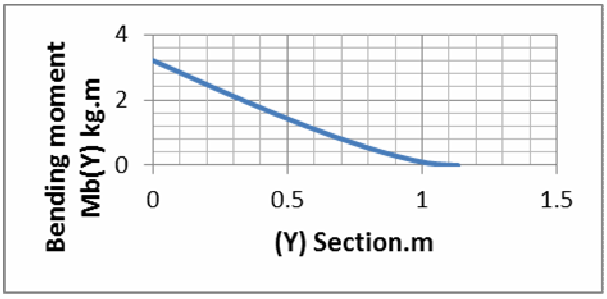

Fig.18. Span-wise bending moment distribution on vertical tails.

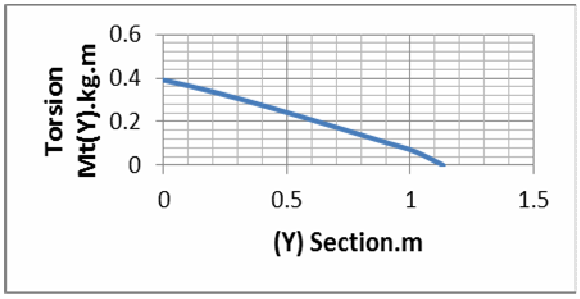

Fig.19. Span-wise torsion moment distribution on vertical tails.

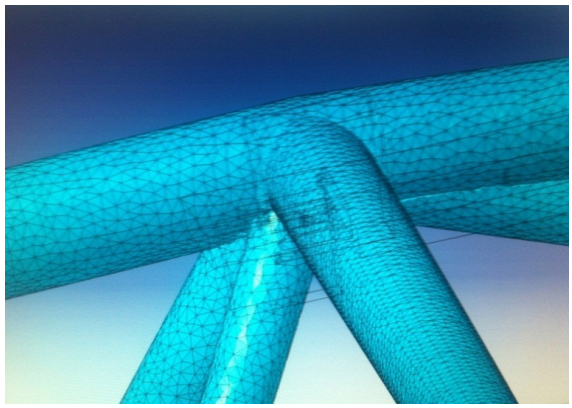

Fig.20. Size of mesh.

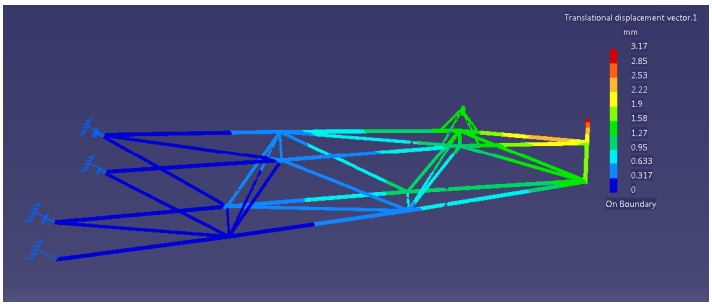

Fig.21. Displacement vector.

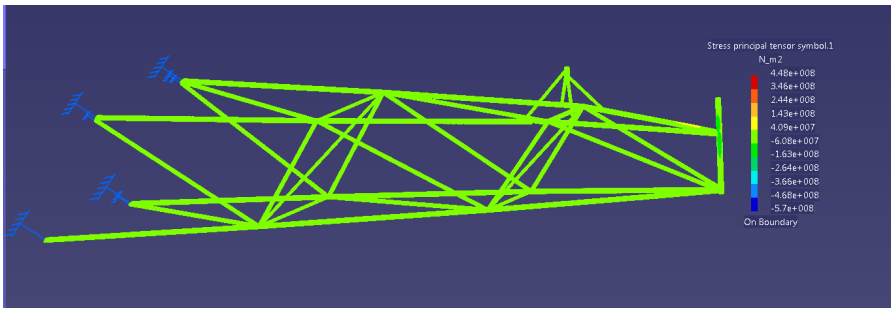

Fig.22. Stress principal tensor.

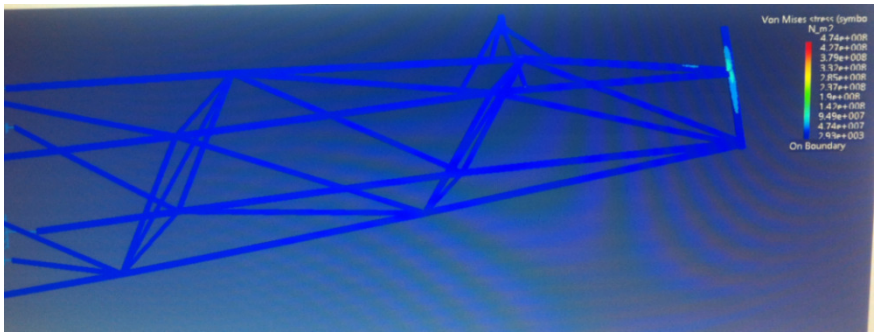

Fig.23. Von Mises stress.

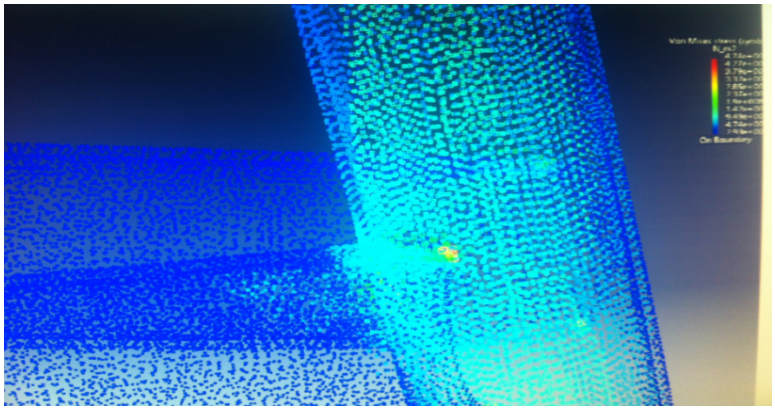

Fig.24. stress concentration spot.

.